Research Article Vol. 5, No. 5 / 15 May 2026 / Optics Continuum 1426

OPTICS CONTINUUM

Gas temperature measurements through broadband femtosecond nitric oxide laser-induced fluorescence in low temperature plasmas

GERARDO URDANETA RINCON,[1,*] LOGAN BYROM,[1] MRUTHUNJAYA UDDI,[2] AND ARTHUR DOGARIU[1,3]

[1]Department of Aerospace Engineering, Texas A&M University, 710 Ross St., College Station, TX 77843, USA
[2]Advanced Cooling Technologies Inc., 1046 New Holland Ave Building 2 Lancaster, PA 17601, USA
[3]Department of Mechanical and Aerospace Engineering, Princeton University, Olden St., Princeton, NJ 08544, USA
[*]gerardo12@tamu.edu

Abstract: This study demonstrates the use of nitric oxide (NO) laser-induced fluorescence (LIF) to measure gas temperature using femtosecond (fs) laser pulses. The technique is established by temperature measurements in a low pressure (100 – 1700 mTorr) gas phase over the surface of a thermocouple monitored resistive wire, as well as in a low-pressure non-equilibrium plasma. A broadband fs laser was tuned to excite several rovibrational NO A-X (0, 0) transitions at the Center Wavelengths (CWLs) of 225 nm and 227 nm to collect their respective LIF signals. It is shown that the ratio of LIF signals at these two CWLs can be used for gas thermometry. LIFBASE simulations were used to identify the sensitive CWLs for temperature measurements. The experiments were conducted in two stages. Firstly, a linear relation between the ratio of LIF signals at 225 nm and 227 nm from the gas phase (2 % NO+N_2) as a function of the thermocouple measured temperature is established experimentally for the 300 – 600 K range. Secondly, it is shown that the temperature measurements obtained by the NO LIF ratio closely agree with the hot wire temperature setpoint in a low pressure non-equilibrium air Capacitively-coupled plasma. The present work shows that fs NO LIF can be reliably used to measure gas temperature to study plasma-surface interactions.

1. Introduction

Non-intrusive, time and spatially resolved in-situ temperature measurements are crucial for studying various physical phenomena, including low-temperature plasmas, combustion, and hypersonics. They are also essential for validating different computational fluid and chemical models. There are several laser techniques used to measure flow temperatures, such as Coherent Anti-Stokes Raman Scattering (CARS) [1–4], spontaneous Rotational Raman Scattering (RRS) [5], Rayleigh Scattering (RS) [6], and laser-induced fluorescence (LIF) [7–14]. LIF-based approaches for measuring temperature and number density offer several advantages, including experimental simplicity, strong signal generation with low pulse energies, applicability across a wide pressure range, and the capability to provide two-dimensionally resolved measurements [15–17]. Methods such as CARS, RRS, and RS demand complex beam alignment, high pulse energies, or suffer signal weakness at low pressures.

Nitric oxide (NO) has been used to measure temperature in reacting flows through either one- or two-Line LIF thermometry [9,13,18]. One-line thermometry utilizes a narrow-band laser to excite a single transition within the NO A-X (0,0) system; while straightforward, this method necessitates the assumption of constant pressure and NO concentration. Conversely, two-line

#591419 https://doi.org/10.1364/OPTCON.591419
Journal © 2026 Received 23 Jan 2026; revised 24 Mar 2026; accepted 14 Apr 2026; published 28 Apr 2026

OPTICS CONTINUUM

thermometry excites two distinct rovibrational transitions, which mitigates these constraints and allows for accurate measurements under fluctuating conditions. However, the efficacy of the two-line approach depends on selecting transitions free from spectral interference, a task that becomes increasingly complex in multi-species environments or when pressure broadening becomes an issue. The use of narrow line width (<0.06 nm) nanosecond (ns) lasers traditionally enabled sensitive LIF measurements, especially at lower pressures where LIF signals are stronger with less interference from neighboring LIF lines. In contrast, femtosecond (fs) lasers, with their broader line widths, can simultaneously excite multiple rovibrational transitions within the NO A–X $(0, 0)$ system, reducing reliance on a single transition and enhancing overall signal robustness. Therefore, it becomes possible to measure temperature by selecting two center wavelengths (CWLs) that are apart enough and vary with temperature. Fs lasers can provide further benefits compared to traditional ns laser techniques, such as more precise quenching rate measurements across a wider pressure range and higher repetition rates [19]. Another advantage of using a fs laser system is the ability to perform simultaneous measurements of multiple species using a single broadband pulse [20]. Compared to other diagnostic techniques, fs NO LIF allows for a simpler experimental setup. Despite the aforementioned benefits, literature regarding fs NO LIF has been limited [20–23].

The purpose of this work is to demonstrate temperature measurements using a broadband ($\sim$ 0.86 nm) fs laser through NO LIF. In this study, fs pulses non-simultaneously excite the NO A-X $(0, 0)$ system at the CWLs of 225 nm and 227 nm and their respective LIF signals are collected. It is shown that the ratio between the LIF signals (S_{225}/S_{227}) is highly sensitive to temperature. The use of broadband fs pulses offer the advantage of reducing quenching effects during the excitation process. This rapid excitation is particularly beneficial compared to ns pulses when the effective excited-state lifetime is on the order of, or shorter than, the duration of a ns pulse. We first demonstrate the sensitivity of the NO LIF signal ratio (LSR) S_{225}/S_{227} to thermocouple-measured temperature over a heating wire. We then show that the temperature obtained using the S_{225}/S_{227} LSR from an Capacitively-coupled air plasma confirms the readings obtained from the thermocouple.

2. Experimental methods

Figure 1 illustrates a schematic of the experimental setup. This experiment is comprised of two stages. In the first stage, a resistor (0.5 mm diameter Kanthal wire) powered by a HY3003-3 direct current power supply and a thermocouple are used to heat a 2% NO + N_2 gas mixture within a cell to a measured temperature. The cell was equipped with 1 mm thick uncoated UV fused silica Thorlabs optical windows (WG41010) to maximize trasmission efficiency in the UV regime. An Edwards nXDS20i Vacuum Pump maintained the cell pressure between 100 – 1700 mTorr. The glass cell was a cylinder 10 in long and 1 in in diameter. These low pressures ensure that our medium can be treated as optically thin. A fs pulse was sequentially tuned between two different wavelengths, 225 nm and 227 nm, to non-simultaneously excite the NO A-X $(0, 0)$ system at a given steady-state condition. S_{225} and S_{227} are the collected LIF signals with CWLs at 225 nm and 227 nm, respectively. The LIF signals are normalized to laser pulse energies. The LSR, S_{225}/S_{227}, was taken for different temperatures to establish a calibration curve. As seen in Fig. 9(a), the ratio of these signals was found to increase linearly with gas temperature for the explored range (300 – 600 K). The second stage involves a Capacitively-coupled radio frequency (RF) low temperature plasma (LTP) to demonstrate that precise gas temperature measurements can be achieved using this technique through the calibration curve. The Capacitively-coupled LTP was generated by a 13.56 MHz signal, which is amplified and adjusted through a matching network. The signal is generated by a Rohde & Schwarz signal generator, amplified by an EIN 325LA RF Power Amplifier, and matched by an MFJ Intellituner. This system can supply up to

OPTICS CONTINUUM

50 W of forward power into the plasma. The gas mixture used was air at the 100 – 1700 mTorr pressure range and the NO was produced chemically.

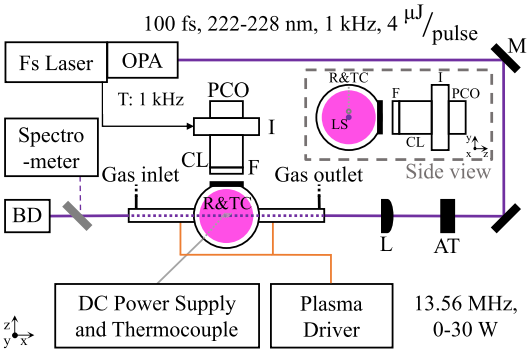

Fig. 1. Experimental setup diagram. AT, attenuator. BD, beam dump. CL, collection lens. F, filter. I, intensifier. L, lens. LS, laser spot. M, mirror. OPA, optical parametric amplifier. PCO, camera. R&TC, resistor and thermocouple. The inset diagram presents a side view of the experiment. The plasma-on condition and resistor are run separately.

A Spectra-Physics Solstice Ace fs laser system operating at 800 nm and 1 kHz repetition rate was adjusted to a range of 222 – 228 nm using a TOPAS Prime and Niruvis optical parametric amplifier to excite the NO A-X $(0, 0)$ transition. The fs pulse was focused with a UV fused silica plano-convex lens with a focal length of 25 cm ($f/25$). The laser beam had a beam spot of 1 cm before reaching the focusing lens. The pulse energy was controlled using a UV fused silica variable neutral density filter as a laser attenuator. A Teledyne HRS-500 spectrometer was used to record the excitation wavelength and account for any power changes resulting from the changing wavelength settings. The IntelliCAL mercury lamp system was employed to calibrate the spectrometer. Detection was performed using a Pco.Edge 5.5 Camera and a gated Stanford Computer Optics Quantum Leap dual-stage intensifier. These were equipped with a CERCO UV lens ($f/2.8$) and a 50 mm-diameter Edmund Optics bandpass filter centered at 253 nm with a bandwidth of 40 nm and a ≥ 4 optical density to capture the NO LIF signal. These LIF signals are normalized to their respective laser pulse energies. A spatial resolution of ~ 12 μm/px was achieved. The fs pulse occurred at $t = 0$ ns, and the intensifier had a gate duration of $\tau_{\text{gate}} = 14$ ns. The intensifier gate was chosen to be much shorter than the NO A-X $(0, 0)$ effective lifetime. The intensifier was triggered at 1 kHz by the fs laser system, and a 1 ns intensifier delay relative to the fs pulse arrival was chosen to avoid laser Rayleigh scattering. This gate-delay configuration was selected to ensure that the method remains independent of quenching effects. The camera was run internally at a frequency of 10 Hz collecting 100 intensifier shots per exposure. A single frame consisted of 32 camera exposures. Therefore, each camera frame contained 3200 laser shots (3.2 s). For each condition tested, a region of interest (ROI) measuring 9.6 mm along the laser propagation direction and 1.32 mm in height was selected (Fig. 2). Spatial averaging was performed across this ROI. To capture the maximum laser intensity value at each horizontal position x, a Gaussian profile was fit to each ROI column (across rows), and the fit peak was used, as shown in Fig. 3. These peak values were then averaged along the horizontal x direction. While spatial averaging was employed to focus solely on the relation between LSR and temperature, it is important to note that the technique is still capable of providing one- and two-dimensionally resolved measurements.

The NO LIF signal as a function of laser energy was measured to ensure the pulse energy was in the linear LIF regime, this is shown in Fig. 4. The air LTP was set to 120 mTorr and 30 W of supplied power. The 226 nm laser energy was varied from 1.8 to 11.9 μJ, and their

OPTICS CONTINUUM

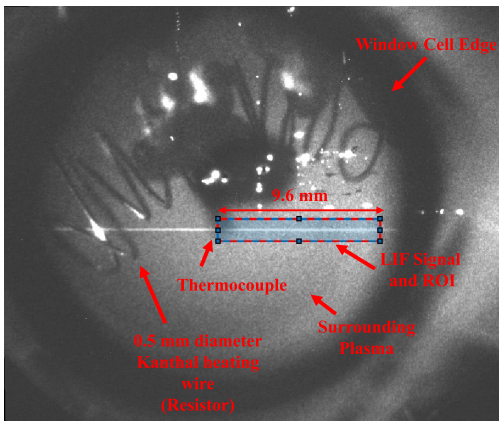

Fig. 2. Image showing the collected laser-induced fluorescence signal excited at center wavelength 225 nm, with the indicated region of interest. The image was obtained with the plasma on and no resistor configuration, at a pressure of $P = 790 \pm 10$ mTorr and a supplied power of 20 W.

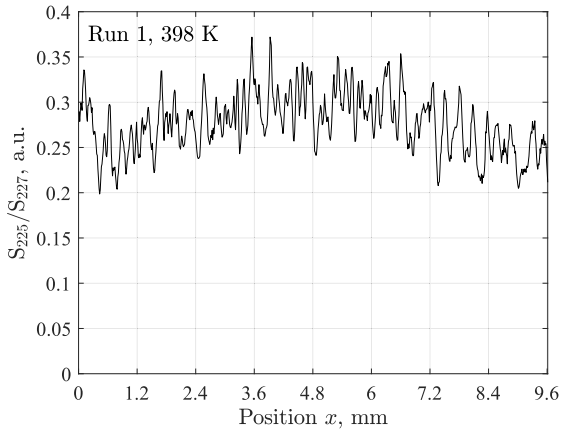

Fig. 3. Laser-induced fluorescence signal ratio (LSR, S_{225}/S_{227}) along the laser propagation direction for Run 1 at thermocouple temperature $T_{\text{tc}} = 398$ K.

respective NO LIF signals were recorded. The NO LIF signal as a function of pulse energy was recorded to determine saturation of the transition. An energy of 4 μJ per pulse was selected for the measurements shown in this work, a value that falls within the LIF linear regime (see Fig. 4). The laser pulse energy was measured with an Edmund Optics 89-310 silicon power detector. The collected NO LIF signal over the 233 – 273 nm spectral range exhibited a decay lifetime of approximately 175 ns (Fig. 5). This value is in line with the 206 ns reported in earlier studies [24]. To minimize quenching effects, the pressure was maintained at 115 mTorr. Based on the decay lifetime, a 14 ns intensifier gate was selected to balance signal accumulation and temporal resolution. This gate width was short enough given the relatively long fluorescence lifetime, allowing sufficient signal integration while mitigating the impact of collisional quenching.

OPTICS CONTINUUM

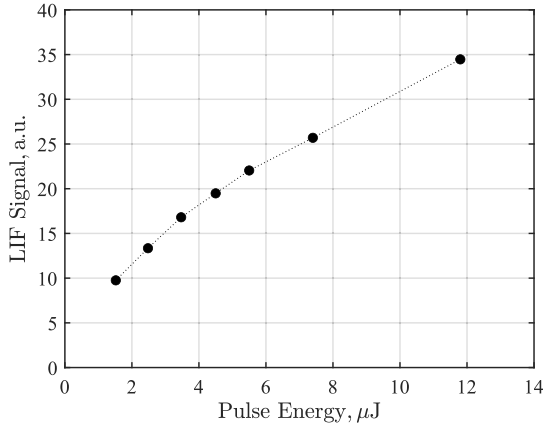

Fig. 4. NO Laser-induced fluorescence (LIF) signal as a function of pulse energy. Air low temperature plasma condition: $P = 120 \pm 10$ mTorr at a supplied power of 30 W. Transition to saturation of the pumped NO LIF line is observed after a pulse energy of 5 μJ.

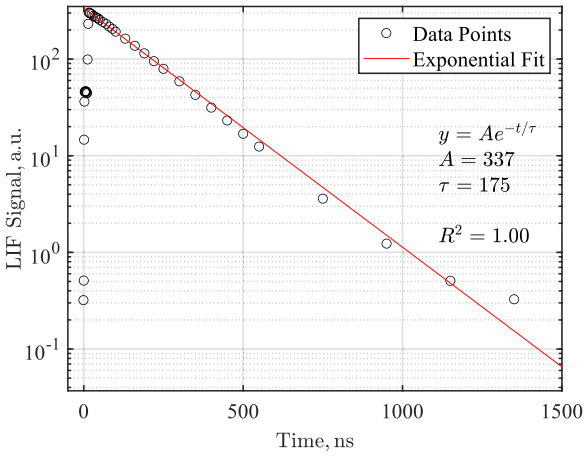

Fig. 5. NO laser-induced fluorescence (LIF) signal decay at a pressure of $P = 115 \pm 10$ mTorr. The observed lifetime of the NO LIF signal is 175 ns.

3. Results and discussion

3.1. Central wavelengths

LIFBASE was used to simulate the accumulated LIF emission (233 − 273 nm) for the NO A-X (0, 0) system at a pressure of 1000 mTorr for various temperatures [25]. Figure 7(a) illustrates the simulated NO LIF signal at 300 K as a function of an idealized delta-function excitation wavelength. Figure 7(b) presents the simulated LIF signal for temperatures of 300 K, 600 K, and 900 K as a function of an idealized delta-function excitation wavelength after being convolved with the fs pulse spectral profile. The curves shown in Fig. 7(b) were obtained from those in Fig. 7(a) (600 K and 900 K not shown) by convolving them with the fs pulse spectral profile, which was modeled as a Gaussian with a bandwidth of 0.86 nm FWHM [26]. While a higher laser bandwidth decreases temperature sensitivity (shallower slope in Fig. 9(a)), it also provides greater resilience by covering a broader range of transition lines. The curves were normalized to the 227 nm CWL because the slope remains unchanged across all temperatures. This makes

OPTICS CONTINUUM

the 227 nm CWL a reliable reference for temperature sensitive LIF signal comparison with the collected LIF signal at the 225 nm CWL. Figure 7(b) shows that the LIF signal level and slope at the 225 nm CWL are sensitive to temperature. Figure 6 shows LIFBASE simulations and experimental results from Run 1 and Run 2 (see Fig. 9), they indicated that the LSRs remained unaffected by pressure across the range investigated in this study. Therefore, this implies that it is possible to tune the fs laser to the 225 nm and 227 nm CWLs, collect their respective LIF signals and obtain a gas temperature measurement from the LSR as long as the pressure remains the same between both measurements.

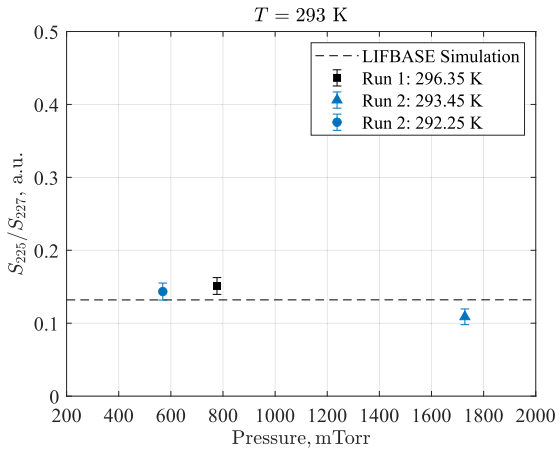

Fig. 6. Dashed line represents the LIFBASE laser-induced fluorescence signal ratio (LSR, S_{225}/S_{227}) as a function of pressure for a temperature of 293 K. Data points indicate the LSR values at various pressure conditions under room temperature. The horizontal trend indicates that LSR is not a function of pressure.

The simulated and convolved curves from Fig. 7(b) are qualitatively compared with the experimentally obtained profiles shown in Fig. 8. Figure 8 presents the experimentally obtained LIF signal profiles for two LTP power conditions (16 W and 30 W) and a reference case without LTP (room temperature). The profiles were measured using an air-flow for the LTP cases and a 2% NO mixture at room temperature for the no-LTP condition. The pressure for all three cases in Fig. 8 was maintained between 105 − 125 mTorr. The red arrow in Fig. 8 highlights the trend of increasing LIF signal at the 225 nm CWL, as shown in the simulated profiles in Fig. 7(b), with increasing temperature. Therefore, from Fig. 8 we experimentally observe that a higher LSR is obtained with increasing gas temperatures (higher supplied power).

3.2. *Temperature measurements*

Figure 9(a) shows the LSR as a function of thermocouple-measured temperatures. The black squares and blue triangles represent data points obtained using the 2 % NO mixture with the heating resistor (no LTP) for Run 1 and Run 2, respectively. Run 1 and Run 2 were conducted on separate occasions, with Run 1 using a single frame containing 3200 laser shots, and Run 2 using four frames, each accumulating 3200 laser shots. For a single frame comprising 3200 laser shots, the signal-to-noise ratio (SNR) was estimated to be approximately ~ 500 for CWL 227 nm and ~ 230 for CWL 225 nm. The error bars represent the 1σ uncertainty and $\bar{\sigma}_{y_i}$ denotes the LSR mean standard deviation, calculated by averaging the standard deviations from both Run 1 and Run 2 data points. Run 1 and Run 2 data sets sample distinct temperature conditions. As a result, they appear differently distributed along the horizontal axis. This approach was taken to avoid redundancy and to improve the robustness of the resulting calibration curve. The pressure range

OPTICS CONTINUUM

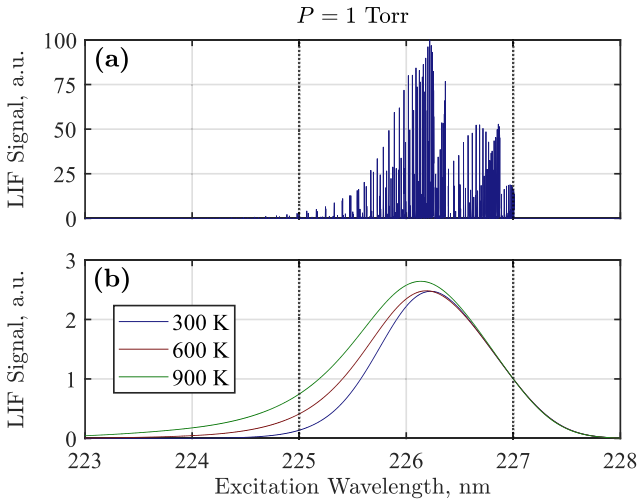

Fig. 7. a) LIFBASE Simulated NO laser-induced fluorescence (LIF) signal as a function of an idealized delta-function excitation wavelength at 300 K. b) Simulated NO LIF signals at 300 K, 600 K, and 900 K using LIFBASE, shown as a function of an idealized delta-function excitation wavelength after being convolved with a 0.86 nm FWHM femtosecond laser profile. All simulations were performed at a pressure of P = 1000 mTorr. The increase in the LIF signal at 225 nm with temperature suggests that the ratio of the LIF signals at 225 nm and 227 nm is temperature dependent.

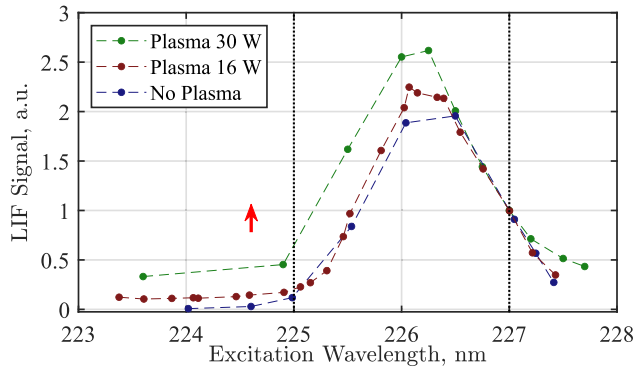

Fig. 8. Collected laser-induced fluorescence (LIF) signal as a function of laser excitation wavelength at different operating conditions. Curves are normalized at 227 nm, and measurements were performed at a pressure of P = 115 ± 10 mTorr. The dashed lines are for illustration purposes only. The increase in the LIF signal at 225 nm with plasma power suggests that the ratio of the LIF signals at 225 nm and 227 nm is temperature dependent.

in Fig. 9(a) was 500 − 1700 mTorr. The broad variation is attributed to thermal expansion of the glass cell from resistor heating, which induces slow pressure fluctuations on the timescale of minutes. This is not expected to impact the results, as the fluorescence signals (S_{225} and S_{227}) for each temperature condition were acquired under constant pressure. The current through the resistor was varied and the gas temperature was measured with the thermocouple, while the LIF signals at 225 nm CWL and 227 nm CWL were captured to obtain the LSR. A linear fit was applied to the blue and black data points. The linear fit parameters—slope a and offset b—are shown, along with the fit metrics: coefficient of determination R^2 and root mean square error

OPTICS CONTINUUM

RMSE. Using the mean standard deviation $\bar{\sigma}_{y_i}$ and the slope of the calibration curve a, the average temperature uncertainty can be estimated via error propagation as $\bar{\sigma}_T = \bar{\sigma}_{y_i}/a \approx 34$ K. Furthermore, the fact that the coefficient of determination is R^2>0.9 in the fit indicates that this relation is close to linear in the explored range (300 – 600 K). It is important to note that this trend may not persist at higher temperatures; however, further studies are required to reveal its behavior. Lastly, it should be noted that radiative heat transfer contributes to the thermal balance of the thermocouple in both the presence and absence of a discharge; consequently, these radiative exchanges represent a non-negligible component of the overall measurement uncertainty.

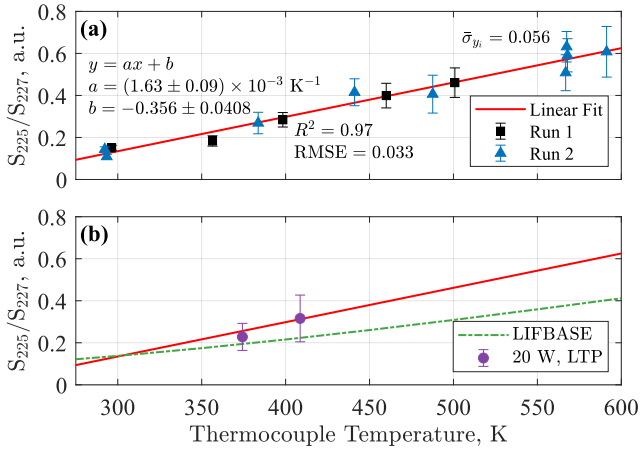

Fig. 9. a) Laser-induced fluorescence (LIF) signal ratio (LSR, S_{225}/S_{227}) as a function of thermocouple-measured temperatures for the resistor-heated 2 % NO + N_2 gas mixture cases, measured at a pressure range of 500 – 1700 mTorr, without the low temperature plasma (LTP). b) Comparison between the calibration curve obtained from Fig. 9(a), LIFBASE simulated curve, and LTP cases, measured at a pressure of P = 790 ± 10 mTorr. The close agreement between the LTP data and the calibration curve demonstrates that femtosecond NO LIF can be used to measure gas temperature in LTPs.

Figure 9(b) shows the LSR as a function of thermocouple-measured temperature. The calibration curve shown in this graph was obtained from the linear fit in Fig. 9(a). The purple circles in Fig. 9(b) were obtained using the air flowed LTP at 20 W, 790 ± 10 mTorr with the gas temperature being measured using the thermocouple; the heating resistor was not employed and the NO was produced chemically. The LIFBASE-simulated LSR is shown in green. The discrepancy between the LIFSBASE-simulated LSR and the experimentally measured LSR in Fig. 9(b) may stem from limited understanding of broadband fs NO LIF spectroscopy at the CWLs used. Fs pulse can induce strong nonlinearities that can dramatically affect the absorption cross sections of the pumped transitions. Further research is required to investigate this discrepancy. Consequently, we adopted a fully experimental approach to develop the calibration curve during the initial stage of our study. The variations in measured LSRs in Fig. 9 between Run 1 and Run 2 can be attributed to micron-scale, day-to-day shifts in grazing laser alignment due to the dynamic nature of the flowing gas system. The fs laser pulse was aligned at a grazing distance from the thermocouple. Temperature gradients may form normal to the resistor and thermocouple surfaces, so slight changes in the relative positioning of the laser, thermocouple, and cell can explain the observed LSRs and thermocouple uncertainty in Fig. 9. Nonetheless, the fact the LTP data points lie close to the linear fit indicates that it is possible to measure the gas temperature using only the LSR and the calibration curve. The LTP gas temperature was measured to be close to 375 K and 410 K. The accuracy of this method is partially dependent on the density of plasma-generated

OPTICS CONTINUUM

NO(A) molecules and the resulting NO A-X (0, 0) photon yield. On the other hand, the influence of gas composition via quenching is minimized in this study. Specifically, by employing an early detection scheme and low operating pressures, the molecular state is effectively frozen on the timescale of detection. Consequently, the LIF signal remains largely independent of the specific quenching partners present in the gas mixture.

4. Conclusion

The experimental setup detailed in this study demonstrates a method to measure gas temperature using NO LSRs using a broadband fs laser. Initially, a resistor and thermocouple were employed to heat a NO gas mixture, establishing a relationship between the 225 nm CWL and 227 nm CWL LSR (S_{225}/S_{227}) and gas temperature. The experiments ensured precise temperature control, and pressure within the vacuum cell was maintained between 100 – 1700 mTorr. In the second stage, a LTP was used to create variable temperature conditions while keeping the pressure constant. A broadband fs laser system, adjusted to excite the NO A-X (0, 0) transitions, and detection equipment ensured accurate LIF signal excitation and capture.

The results show a linear relationship between the S_{225}/S_{227} LSR and gas temperature for the investigated range (300 – 600 K). Initial tests with varied laser pulse energy showed a consistent linear response, establishing 4 μJ per pulse as optimal for avoiding saturation. Experimental data showed that the LIF signal at the 225 nm CWL (S_{225}) increases with temperature compared to the 227 nm CWL LIF signal (S_{227}). LTP operating conditions closely matched the linear fit derived from the resistor-heated setup, validating this thermometry technique as a practical approach. In conclusion, fs NO LIF can be employed to effectively measure gas temperature in LTPs.

Funding. United States Air Force (F222-0018-0088).

Disclosures. The authors declare no conflicts of interest.

Data Availability. Data underlying the results presented in this paper are not publicly available at this time but may be obtained from the authors upon reasonable request.

References

1. P. D. Maker and R. W. Terhune, "Study of optical effects due to an induced polarization third order in the electric field strength," Phys. Rev. **137**(3A), A801–A818 (1965).
2. T. Lang and M. Motzkus, "Single-shot femtosecond coherent anti-Stokes Raman-scattering thermometry," J. Opt. Soc. Am. B **19**(2), 340 (2002).
3. S. Roy, J. R. Gord, and A. K. Patnaik, "Recent advances in coherent anti-Stokes Raman scattering spectroscopy: gundamental developments and applications in reacting flows," Prog. Energy Combustion Sci. **36**(2), 280–306 (2010).
4. A. Farooq, A. B. Alquaity, M. Raza, *et al.*, "Laser sensors for energy systems and process industries: perspectives and directions," Prog. Energy Combustion Sci. **91**, 100997 (2022).
5. B. L. Klarenaar, M. Grofulović, A. S. Morillo-Candas, *et al.*, "A rotational Raman study under non-thermal conditions in a pulsed CO_2 glow discharge," Plasma Sources Sci. Technol. **27**(4), 045009 (2018).
6. J. Haumann and A. Leipertz, "Flame-temperature measurements using the Rayleigh scattering photon-correlation technique," Opt. Lett. **9**(11), 487 (1984).
7. D. Zelenak and V. Narayanaswamy, "Demonstration of a two-line Kr PLIF thermometry technique for gaseous combustion applications," Opt. Lett. **44**(2), 367 (2019).
8. P. S. Hsu, N. Jiang, J. J. Felver, *et al.*, "10 kHz two-color OH PLIF thermometry using a single burst-mode OPO," Opt. Lett. **46**(10), 2308 (2021).
9. M. P. Lee, B. K. McMillin, and R. K. Hanson, "Temperature measurements in gases by use of planar laser-induced fluorescence imaging of NO," Appl. Opt. **32**(27), 5379 (1993).
10. W. G. Bessler, C. Schulz, T. Lee, *et al.*, "Strategies for laser-induced fluorescence detection of nitric oxide in high-pressure flames. I. *A–X*excitation," Appl. Opt. **41**(18), 3547 (2002).
11. A. V. Mokhov, H. B. Levinsky, and C. E. van der Meij, "Temperature dependence of laser-induced fluorescence of nitric oxide in laminar premixed atmospheric-pressure flames," Appl. Opt. **36**(15), 3233 (1997).
12. S. V. Naik, W. D. Kulatilaka, K. K. Venkatesan, *et al.*, "Pressure, temperature, and velocity measurements in underexpanded jets using laser-induced fluorescence imaging," AIAA J. **47**(4), 839–849 (2009).
13. C. M. Loe, J. D. Winner, and R. Sánchez-González, "Thermometry in gas flows using two-line fluorescence imaging and structured illumination," OSA Continuum **1**(4), 1185 (2018).
14. C. Schulz, V. Sick, J. Heinze, *et al.*, "Laser-induced-fluorescence detection of nitric oxide in high-pressure flames with A–X(0, 2) excitation," Appl. Opt. **36**(15), 3227 (1997).

OPTICS CONTINUUM

15. J. Heinze, U. Meier, T. Behrendt, *et al.*, "PLIF thermometry based on measurements of absolute concentrations of the OH radical," Zeitschrift fur Physikalische Chemie **225**(11-12), 1315–1341 (2011).
16. H. Wei, H. Du, G. Zhou, *et al.*, "Temperature measurements of ammonia-hydrogen laminar diffusion flames by two-color NO-PLIF," Int. J. Hydrogen Energy **58**, 931–940 (2024).
17. A. M. Webb, C. Q. Crabtree, V. Athmanathan, *et al.*, "High-efficiency narrow-bandwidth KTP optical parametric oscillator for kHz–MHz planar laser-induced fluorescence," Opt. Lett. **49**(6), 1473 (2024).
18. D. C. Van Den Bekerom, E. R. Jans, and I. V. Adamovich, "NO PLIF flow visualization and time-resolved temperature distributions in laser induced breakdown plumes," J. Phys. D: Appl. Phys. **54**(26), 265201 (2021).
19. J. B. Schmidt, B. Sands, J. Scofield, *et al.*, "Comparison of femtosecond- and nanosecond-two-photon-absorption laser-induced fluorescence (TALIF) of atomic oxygen in atmospheric-pressure plasmas," Plasma Sources Sci. Technol. **26**(5), 055004 (2017).
20. M. Hay, P. Parajuli, and W. D. Kulatilaka, "Simultaneous detection of three chemical species (NO, O, O_2) using a single broadband femtosecond laser," Proc. Combust. Inst. **39**(1), 1435–1444 (2023).
21. A. V. Puchikin, Y. N. Panchenko, S. A. Yampolskaya, *et al.*, "Laser-induced fluorescence of vibrationally excited nitric oxide by femtosecond laser pulse," J. Lumin. **268**, 120412 (2024).
22. G. A. Urdaneta, L. Byrom, M. Uddi, *et al.*, "Temperature measurements through femtosecond nitric oxide laser induced fluorescence," in *AIAA SciTech Forum 2025*, (AIAA Inc, 2025).
23. M. K. Hay, M. Suarez, and W. D. Kulatilaka, "1D flame thermometry using femtosecond LIF of NO," in *AIAA SciTech Forum 2025*, (AIAA Inc, 2025).
24. J. Luque and D. R. Crosley, "Transition probabilities and electronic transition moments of the $A^2\Sigma+ - X^2\Pi$ and $D^2\Sigma+ - X^2\Pi$ systems of nitric oxide," J. Chem. Phys. **111**(16), 7405–7415 (1999).
25. Luque Jorge and Crosley David, "LIFBASE: database and spectral simulation program," SRI International Report MP (1999).
26. M. Tamura, J. Luque, J. E. Harrington, *et al.*, "Laser-induced fluorescence of seeded nitric oxide as a flame thermometer," Appl. Phys. B: Lasers Opt. **66**(4), 503–510 (1998).